

AD-A032 081

OAKLAND UNIV ROCHESTER MICH SCHOOL OF ENGINEERING

F/G 20/11

TIME-AVERAGED SHADOW-MOIRE METHOD FOR STUDYING VIBRATIONS, (U)

NOV 76 Y Y HUNG, C Y LIANG, J D HOVANESIAN

N00014-76-C-0487

UNCLASSIFIED

39

NL

1 OF 1
ADA032081



END

DATE
FILMED

1 - 77

AD A032081

TIME-AVERAGED SHADOW MOIRÉ METHOD
FOR STUDYING VIBRATIONS

BY

Y. Y. HUNG, C. Y. LIANG, J. D. HOVANESIAN AND A. J. DURELLI

SPONSORED BY

OFFICE OF NAVAL RESEARCH
DEPARTMENT OF THE NAVY
WASHINGTON, D.C. 20025

AND

NATIONAL SCIENCE FOUNDATION
WASHINGTON, D.C. 20550

SCHOOL OF ENGINEERING
OAKLAND UNIVERSITY
ROCHESTER, MICHIGAN 48063

NOVEMBER 1976



DISTRIBUTION STATEMENT A

Approved for public release
Distribution Unlimited

6 TIME-AVERAGED SHADOW-MOIRE METHOD
FOR STUDYING VIBRATIONS

by

10 Y. Y./Hung, C. Y./Liang, J. D./Hovanesian and A. J./Durelli

Sponsored by

Office of Naval Research
Department of the Navy
Washington, D.C. 20025

15 ON C-
Contract No. N00014-76-0487
O.U. Project No. 38472-86
Report No. 39
14

National Science Foundation
Washington, D.C. 20550

on NSF-
Grant No. ENG-76-08751
O.U. Project No. 38510-24

School of Engineering
Oakland University
Rochester, Michigan 48063

11 November 1976

12 22p.

ACCESSION for	
NTIS	White Section <input checked="" type="checkbox"/>
DDC	Buff Section <input type="checkbox"/>
UNANNOUNCED	<input type="checkbox"/>
JUSTIFICATION	
BY	
DISTRIBUTION/AVAILABILITY CODES	
Dist.	AVAIL. and/or SPECIAL
A	

1473

Imma

405252

TIME-AVERAGED SHADOW-MOIRÉ METHOD
FOR STUDYING VIBRATIONS

by

Y. Y. Hung, C. Y. Liang, J. D. Hovanesian and A. J. Durelli

ABSTRACT

A time-averaged shadow-moiré method is presented which permits the determination of the amplitude distribution of the deflection of a plate in steady state vibration. No stroboscope is required and the recording is done statically. The method is less sensitive than holographic methods and is therefore suitable for studying relatively large amplitudes.

Previous Technical Reports to the Office of Naval Research

1. A. J. Durelli, "Development of Experimental Stress Analysis Methods to Determine Stresses and Strains in Solid Propellant Grains"--June 1962. Developments in the manufacturing of grain-propellant models are reported. Two methods are given: a) cementing routed layers and b) casting.
2. A. J. Durelli and V. J. Parks, "New Method to Determine Restrained Shrinkage Stresses in Propellant Grain Models"--October 1962. The birefringence exhibited in the curing process of a partially restrained polyurethane rubber is used to determine the stress associated with restrained shrinkage in models of solid propellant grains partially bonded to the case.
3. A. J. Durelli, "Recent Advances in the Application of Photoelasticity in the Missile Industry"--October 1962. Two- and three-dimensional photoelastic analysis of grains loaded by pressure and by temperature are presented. Some applications to the optimization of fillet contours and to the redesign of case joints are also included.
4. A. J. Durelli and V. J. Parks, "Experimental Solution of Some Mixed Boundary Value Problems"--April 1964. Means of applying known displacements and known stresses to the boundaries of models used in experimental stress analysis are given. The application of some of these methods to the analysis of stresses in the field of solid propellant grains is illustrated. The presence of the "pinching effect" is discussed.
5. A. J. Durelli, "Brief Review of the State of the Art and Expected Advance in Experimental Stress and Strain Analysis of Solid Propellant Grains"--April 1964. A brief review is made of the state of the experimental stress and strain analysis of solid propellant grains. A discussion of the prospects for the next fifteen years is added.
6. A. J. Durelli, "Experimental Strain and Stress Analysis of Solid Propellant Rocket Motors"--March 1965. A review is made of the experimental methods used to strain-analyze solid propellant rocket motor shells and grains when subjected to different loading conditions. Methods directed at the determination of strains in actual rockets are included.
7. L. Ferrer, V. J. Parks and A. J. Durelli, "An Experimental Method to Analyze Gravitational Stresses in Two-Dimensional Problems"--October 1965. Photoelasticity and moiré methods are used to solve two-dimensional problems in which gravity-stresses are present.

8. A. J. Durelli, V. J. Parks and C. J. del Rio, "Stresses in a Square Slab Bonded on One Face to a Rigid Plate and Shrunk"--November 1965.
A square epoxy slab was bonded to a rigid plate on one of its faces in the process of curing. In the same process the photoelastic effects associated with a state of restrained shrinkage were "frozen-in." Three-dimensional photoelasticity was used in the analysis.
9. A. J. Durelli, V. J. Parks and C. J. del Rio, "Experimental Determination of Stresses and Displacements in Thick-Wall Cylinders of Complicated Shape"--April 1966.
Photoelasticity and moiré are used to analyze a three-dimensional rocket shape with a star shaped core subjected to internal pressure.
10. V. J. Parks, A. J. Durelli and L. Ferrer, "Gravitational Stresses Determined Using Immersion Techniques"--July 1966.
The methods presented in Technical Report No. 7 above are extended to three-dimensions. Immersion is used to increase response.
11. A. J. Durelli and V. J. Parks. "Experimental Stress Analysis of Loaded Boundaries in Two-Dimensional Second Boundary Value Problems"--February 1967.
The pinching effect that occurs in two-dimensional bonding problems, noted in Reports 2 and 4 above, is analyzed in some detail.
12. A. J. Durelli, V. J. Parks, H. C. Feng and F. Chiang, "Strains and Stresses in Matrices with Inserts,"-- May 1967.
Stresses and strains along the interfaces, and near the fiber ends, for different fiber end configurations, are studied in detail.
13. A. J. Durelli, V. J. Parks and S. Uribe, "Optimization of a Slot End Configuration in a Finite Plate Subjected to Uniformly Distributed Load,"--June 1967.
Two-dimensional photoelasticity was used to study various elliptical ends to a slot, and determine which would give the lowest stress concentration for a load normal to the slot length.
14. A. J. Durelli, V. J. Parks and Han-Chow Lee, "Stresses in a Split Cylinder Bonded to a Case and Subjected to Restrained Shrinkage,"--January 1968.
A three-dimensional photoelastic study that describes a method and shows results for the stresses on the free boundaries and at the bonded interface of a solid propellant rocket.
15. A. J. Durelli, "Experimental Stress Analysis Activities in Selected European Laboratories"--August 1968.
This report has been written following a trip conducted by the author through several European countries. A list is given of many of the laboratories doing important experimental stress analysis work and of the people interested in this kind of work. An attempt has been made to abstract the main characteristics of the methods used in some of the countries visited.

16. V. J. Parks, A. J. Durelli and L. Ferrer, "Constant Acceleration Stresses in a Composite Body"--October 1968.
Use of the immersion analogy to determine gravitational stresses in two-dimensional bodies made of materials with different properties.
17. A. J. Durelli, J. A. Clark and A. Kochev, "Experimental Analysis of High Frequency Stress Waves in a Ring"--October 1968.
A method for the complete experimental determination of dynamic stress distributions in a ring is demonstrated. Photoelastic data is supplemented by measurements with a capacitance gage used as a dynamic lateral extensometer.
18. J. A. Clark and A. J. Durelli, "A Modified Method of Holographic Interferometry for Static and Dynamic Photoelasticity"--April 1968.
A simplified absolute retardation approach to photoelastic analysis is described. Dynamic isopachics are presented.
19. J. A. Clark and A. J. Durelli, "Photoelastic Analysis of Flexural Waves in a Bar"--May 1969.
A complete direct, full-field optical determination of dynamic stress distribution is illustrated. The method is applied to the study of flexural waves propagating in a urethane rubber bar. Results are compared with approximate theories of flexural waves.
20. J. A. Clark and A. J. Durelli, "Optical Analysis of Vibrations in Continuous Media"--June 1969.
Optical methods of vibration analysis are described which are independent of assumptions associated with theories of wave propagation. Methods are illustrated with studies of transverse waves in prestressed bars, snap loading of bars and motion of a fluid surrounding a vibrating bar.
21. V. J. Parks, A. J. Durelli, K. Chandrashekhara and T. L. Chen, "Stress Distribution Around a Circular Bar, with Flat and Spherical Ends, Embedded in a Matrix in a Triaxial Stress Field"--July 1969.
A Three-dimensional photoelastic method to determine stresses in composite materials is applied to this basic shape. The analyses of models with different loads are combined to obtain stresses for the triaxial cases.
22. A. J. Durelli, V. J. Parks and L. Ferrer, "Stresses in Solid and Hollow Spheres Subjected to Gravity or to Normal Surface Traction"--October 1969.
The method described in Report No. 10 above is applied to two specific problems. An approach is suggested to extend the solutions to a class of surface traction problems.
23. J. A. Clark and A. J. Durelli, "Separation of Additive and Subtractive Moiré Patterns"--December 1969.
A spatial filtering technique for adding and subtracting images of several gratings is described and employed to determine the whole field of Cartesian shears and rigid rotations.

24. R. J. Sanford and A. J. Durelli, "Interpretation of Fringes in Stress-Holo-Interferometry"--July 1970.
Errors associated with interpreting stress-holo-interferometry patterns as the superposition of isopachics (with half order fringe shifts) and isochromatics are analyzed theoretically and illustrated with computer generated holographic interference patterns.
25. J. A. Clark, A. J. Durelli and P. A. Laura, "On the Effect of Initial Stress on the Propagation of Flexural Waves in Elastic Rectangular Bars"--December 1970.
Experimental analysis of the propagation of flexural waves in prismatic, elastic bars with and without prestressing. The effects of prestressing by axial tension, axial compression and pure bending are illustrated.
26. A. J. Durelli and J. A. Clark, "Experimental Analysis of Stresses in a Buoy-Cable System Using a Birefringent Fluid"--February 1971.
An extension of the method of photoviscous analysis is presented which permits quantitative studies of strains associated with steady state vibrations of immersed structures. The method is applied in an investigation of one form of behavior of buoy-cable systems loaded by the action of surface waves.
27. A. J. Durelli and T. L. Chen, "Displacements and Finite-Strain Fields in a Sphere Subjected to Large Deformations"--February 1972.
Displacements and strains (ranging from 0.001 to 0.50) are determined in a polyurethane sphere subjected to several levels of diametral compression. A 500 lines-per-inch grating was embedded in a meridian plane of the sphere and moiré effect produced with a non-deformed master. The maximum applied vertical displacement reduced the diameter of the sphere by 27 per cent.
28. A. J. Durelli and S. Machida, "Stresses and Strain in a Disk with Variable Modulus of Elasticity"--March 1972.
A transparent material with variable modulus of elasticity has been manufactured that exhibits good photoelastic properties and can also be strain analyzed by moiré. The results obtained suggests that the stress distribution in the homogeneous disk. It also indicates that the strain fields in both cases are very different, but that it is possible, approximately, to obtain the stress field from the strain field using the value of E at every point, and Hooke's law.
29. A. J. Durelli and J. Buitrago, "State of Stress and Strain in A Rectangular Belt Pulled Over a Cylindrical Pulley"--June 1972.
Two- and three-dimensional photoelasticity as well as electrical strain gages, dial gages and micrometers are used to determine the stress distribution in a belt-pulley system. Contact and tangential stress for various contact angles and friction coefficients are given.

30. T. L. Chen and A. J. Durelli, "Stress Field in a Sphere Subjected to Large Deformations"--June 1972.
Strain fields obtained in a sphere subjected to large diametral compressions from a previous paper were converted into stress fields using two approaches. First, the concept of strain-energy function for an isotropic elastic body was used. Then the stress field was determined with the Hookean type natural stress-natural strain relation. The results so obtained were also compared.
31. A. J. Durelli, V. J. Parks and H. M. Hasseem, "Helices Under Load"--July 1973.
Previous solutions for the case of close coiled helical springs and for helices made of thin bars are extended. The complete solution is presented in graphs for the use of designers. The theoretical development is correlated with experiments.
32. T. L. Chen and A. J. Durelli, "Displacements and Finite Strain Fields in a Hollow Sphere Subjected to Large Elastic Deformations"--September 1973.
The same methods described in No. 27, were applied to a hollow sphere with an inner diameter one half the outer diameter. The hollow sphere was loaded up to a strain of 30 per cent on the meridian plane and a reduction of the diameter by 20 per cent.
33. A. J. Durelli, H. H. Hasseem and V. J. Parks, "New Experimental Method in Three-Dimensional Elastostatics"--December 1973.
A new material is reported which is unique among three-dimensional stress-freezing materials, in that, in its heated (or rubbery) state it has a Poisson's ratio which is appreciably lower than 0.5. For a loaded model, made of this material, the unique property allows the direct determination of stresses from strain measurements taken at interior points in the model.
34. J. Wolak and V. J. Parks, "Evaluation of Large Strains in Industrial Applications"--April 1974.
It was shown that Mohr's circle permits the transformation of strain from one axis of reference to another, irrespective of the magnitude of the strain, and leads to the evaluation of the principal strain components from the measurement of direct strain in three directions.
35. A. J. Durelli, "Experimental Stress Analysis Activities in Selected European Laboratories"--April 1975.
Continuation of Report No. 15 after a visit to Belgium, Holland, Germany, France, Turkey, England and Scotland.
36. A. J. Durelli, V. J. Parks and J. O. Bühler-Vidal, "Linear and Non-linear Elastic and Plastic Strains in a Plate with a Big Hole Loaded Axially in its Plane"--July 1975.
Strain analysis of the ligament of a plate with a big hole indicates that both geometric and material non-linearity may take place. The strain concentration factor was found to vary from 1 to 2 depending on the level of deformation.

37. A. J. Durelli, V. Pavlin, J. O. Bühler-Vidal and G. Ome, "Elastostatics of a Cubic Box Subjected to Concentrated Loads"--August 1975.
Analysis of experimental strain, stress and deflection of a cubic box subjected to concentrated loads applied at the center of two opposite faces. The ratio between the inside span and the wall thickness was varied between approximately 5 and 121.
38. A. J. Durelli, V. J. Parks and J. O. Bühler-Vidal, "Elastostatics of Cubic Boxes Subjected to Pressure"--March 1976.
Experimental analysis of strain, stress and deflections in a cubic box subjected to either internal or external pressure. Inside span-to-wall thickness ratio varied from 5 to 14.

Introduction

Besides its uses in evaluating surface depth contours⁽¹⁻³⁾ and in determining surface deformations,⁽⁴⁻⁸⁾ the shadow moiré method was also used to study nodal patterns in vibrating plates.⁽⁹⁾ However, to study amplitude distribution, a stroboscopic method was required.⁽¹⁰⁾ This paper presents a time-averaged shadow moiré method whereby the distribution of the amplitude of the plate deflection can be obtained without stroboscopic equipment. In the method, the shadow moiré contour fringes of an object in steady state vibration is photographed with an exposure time equal to one or several vibrational periods. The processed photograph produces a time-averaged fringe pattern depicting the vibrational amplitudes.

The time-averaged effect utilized in the present paper was first applied by Powell and Stetson to vibration studies using holography.⁽¹¹⁾ The hologram they obtained recorded the position of a steady state vibrating object with a long exposure time compared to the vibrational period. They showed that in the reconstruction of this hologram a time-averaged interference fringe pattern was produced which measured the vibrational amplitudes. The fringe pattern could be represented mathematically by a zero-order Bessel function. The time-averaged effect was later applied to study vibrations using projected gratings methods.^(12,13) However, the two techniques are on opposite extremes in the range of sensitivities. While the time-averaged holography is extremely sensitive being able to measure vibrational amplitudes of the order of wavelengths of light, the projected gratings methods are rather insensitive. Therefore, there is a large gap in the sensitivity range between the two techniques. The present method, though still unable to bridge the entire gap, has extended the sensitivity of the projected gratings methods.

Description of the Method

The method uses a standard shadow moiré arrangement as shown in Fig. 1. A master grating with lines running parallel to the y-axis is located in front of and close to the object to be studied. A collimated beam of light illuminates the grating at an angle θ to the y,z-plane, and a distant camera views the grating normally.

If the object surface to be studied is flat, it is carefully positioned so that the stationary moiré contour fringes are null. Then with the object being excited to vibrate steadily, a time-dependent moiré fringe pattern due to the vibrational displacements is observed. If the time-varying fringe pattern is recorded by the camera with an exposure time of one or several vibrational periods, the processed photograph will yield a time-averaged fringe pattern which is related to the vibrational amplitudes by a zero-order Bessel function.

For objects which are not flat, it is not possible to null the stationary contour fringes. In this case, it is advisable to use a rather dense initial contour fringe pattern deliberately introduced by slightly tilting the object about an axis perpendicular to the viewing direction. This initial fringe pattern is then used as a carrier which is modulated by the vibrational amplitudes. The time-averaged fringes formed by the modulated carrier also depict the amplitude distribution of the vibration.

If the vibrational frequency is high enough (20 Hz or higher), the image retaining nature of the eye can do the time averaging. Hence, real time averaged moiré fringes may be observed by the naked eye.

Theory of the Method

Assume that the intensity transmittance of the master grating is sinusoidal and represented by:

$$T(x,y) = 1 + \sin \frac{2\pi}{p} x \quad (1)$$

where p is the grating pitch. The obliquely illuminating beam casts a shadow of the grating onto the object surface. Under the condition that the grating is coarse enough for diffraction effects to be neglected, it can be shown that the intensity distribution $I_s(x,y)$ of the shadow is: ⁽¹⁾

$$I_s(x,y) = k \left[1 + \sin \frac{2\pi}{p} (x - z \tan \theta) \right] \quad (2)$$

where k is a constant depending on the scattering attenuation of the object surface and z is the surface elevation.

Since the camera views the shadow through the master ruling, the intensity of the image $I_o(x,y)$ detected is the product of the shadow intensity and the grating transmittance and is given by:

$$I_o(x,y) = I_s(x,y) \cdot T(x,y) \quad (3)$$

Expansion of the above equation yields

$$\begin{aligned} I_o(x,y) = k \left\{ 1 + \sin \frac{2\pi}{p} x + \sin \frac{2\pi}{p} (x - z \tan \theta) \right. \\ \left. + \frac{1}{2} \cos \frac{2\pi}{p} (2x - z \tan \theta) + \frac{1}{2} \cos \left(\frac{2\pi}{p} z \tan \theta \right) \right\} \end{aligned} \quad (4)$$

All the terms on the right-hand side of the above equation are of high spatial frequency which will average to zero, except the following:

$$I_o(x,y) = k \left\{ 1 + \frac{1}{2} \cos \frac{2\pi}{p} z \tan\theta \right\} \quad (5)$$

This equation predicts the formation of moiré fringes depicting z , the contour of the surface.

With the surface undergoing steady state sinusoidal oscillation, z is given by:

$$z = z_o + A(x,y) \cdot \cos(\omega t + \phi) \quad (6)$$

where z_o is the stationary contour of the object surface; $A(x,y)$ is the amplitude distribution of the vibrating surface; ω is the circular frequency, and ϕ represents the arbitrary initial phase. Thus, z in Eq. (5) is time-dependent and $I_o(x,y)$ should be replaced by $I_o(x,y,t)$. If the photographic film in the camera is exposed to $I_o(x,y,t)$ the exposure on the film is an integration of $I_o(x,y,t)$ over the exposure time which can be adjusted to an integral multiple of the vibrational periods. The integrated intensity is $I_i(x,y)$ given by:

$$I_i(x,y) = \int_0^{nT} I_o(x,y,t) dt \quad (7)$$

where nT is the exposure time; n is an integer and T the vibrational period.

Techniques

1. For flat objects:

For a flat object, it is possible to null the stationary contour fringes by positioning the object so that $z_o = \text{constant}$ (i.e., the flat surface is parallel to the plane of the grating). Then Eq. (6) can be integrated to yield:

$$I_o(x,y) = nT \cdot k \cdot \left\{ 1 + \frac{1}{2} \cdot \cos\left(\frac{2\pi}{p} z_o\right) \cdot J_o\left[\frac{2\pi}{p} \tan\theta \cdot A(x,y)\right] \right\} \quad (8)$$

The above equation indicates a fringe pattern depicted by a zero-order Bessel function containing $A(x,y)$, the vibrational amplitude distribution, in its argument. Dark fringes occur when the Bessel function attains its minimum, i.e.

$$\frac{2\pi}{p} \tan\theta \cdot A(x,y) = B_j \quad (9)$$

where B_j is the argument of the j th minimum value of J_o . By rewriting Eq. (9) as

$$A(x,y) = \frac{B_j}{2\pi} \left(\frac{p}{\tan\theta}\right) \quad (10)$$

and defining $\frac{B_j}{2\pi} = N$ as the fringe order, then the amplitude distribution $A(x,y)$ can be determined by the following equation

$$A(x,y) = N \left(\frac{p}{\tan\theta}\right) \quad (11)$$

where $N = 0.610, 1.62, 2.62, 3.62, 4.62, \dots$

2. For arbitrarily curved surfaces

For curved surface it is not possible to null the stationary contours.

In this case, relatively high density fringes are deliberately introduced by slightly rotating (say α) the object about x-axis.

z in Eq. (6) becomes

$$z = (z_o + \alpha y) + A(x,y) \cdot \cos (\omega t + \phi) \quad (12)$$

Equation (9) is then substituted into Eq. (7). Integration of the resulting equation yields

$$I_a(x,y) = 1 + \frac{1}{2} \cos \frac{2\pi}{p} (z_o + \alpha y) \cdot J_o \left[\frac{2\pi}{p} \tan \theta \cdot A(x,y) \right] \quad (13)$$

Equation (13) is an expression where a high frequency term is amplitude modulated by $J_o \left[\frac{2\pi}{p} \tan \theta \cdot A(x,y) \right]$. In this case the nulling of the high frequency term (carrier) is identified as moiré fringes which occur when the Bessel function is equal to zero, i.e., the argument is equal to the roots of the function. It can be shown, by following a similar analysis as in the last section, that the amplitude distribution $A(x,y)$ can be determined by Eq. (10). For this case, $N = \frac{B_j}{2\pi}$ where B_j is the j th root of J_o , and takes the values of 0.383, 0.879, 1.38, 1.88, 2.38,

While the first technique is only applicable to flat objects, the fringe modulation technique can be used for studying objects of both flat and curved surfaces. Our experience shows that fringes of better visibility were obtained using the first technique. However, the fringe modulation technique is better suited for studying nodal patterns.

Similar results will be obtained if the intensity transmittance of the grating is a square function with the advantage that a better fringe visibility can be achieved.

Experiments

A circular rubber membrane of 10 cm diameter clamped along its boundary was selected for demonstration. It was excited into vibration from behind by a loud speaker driven by a wave generator. A one-way grating of 20 lines per centimeter was used. The light source was a projector located at a great distance from the object in a direction making an angle $\theta = 60^\circ$ with the normal to the plate.

The grating was carefully positioned in respect to the plate to avoid any initial interference. The plate was then excited at its natural frequencies of 100 and 185 Hz. The fringe patterns obtained depicting the amplitude distributions of the vibrational modes are shown in Fig. 2.

To demonstrate the fringe carrier technique, the membrane was slightly tilted to produce the initial fringe carrier shown in Fig. 3(A). The time-averaged moiré fringes formed by the fringe carrier when the membrane was excited to vibrate at 100 Hz and 185 Hz are shown in Fig. 3(B) and Fig. 3(C), respectively.

Conclusion

It has been shown that time-averaged shadow moiré fringes are formed when an object is undergoing steady state oscillation. The fringes are loci of

deflection amplitude interpreted by a zeroth order Bessel function. Owing to the fact that the value of the Bessel function decreases as the value of the argument increases, the fringe visibility drops with the increasing amplitude. This provides a means of identifying nodal areas as well as the fringe orders.

In the projected grating method, it is necessary for the imaging system to resolve the grating projected on the object surface. Therefore, the limit to the fineness of the grating that can be projected and recorded bounds the sensitivity of the method. The present method requires only the moiré fringes to be resolved, thus allowing gratings of higher frequency to be used. Hence, it extends the sensitivity range of the projected grating method.

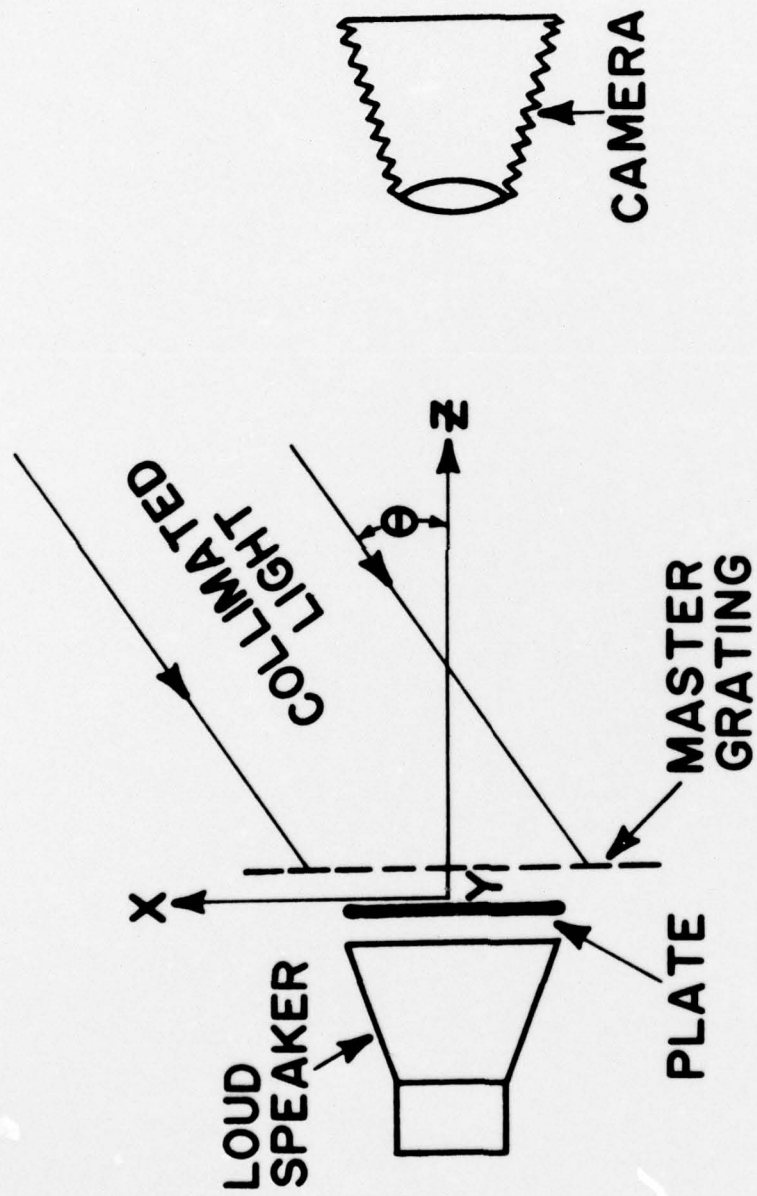
Acknowledgement

The research work reported in this paper was supported financially, in part, by the National Science Foundation (Grant ENG 76-08751), and the Office of Naval Research (Contract No. N-00014-76-C-0487). The authors are very grateful to C. J. Astill and N. Perrone, monitors of the program, for their support.

References

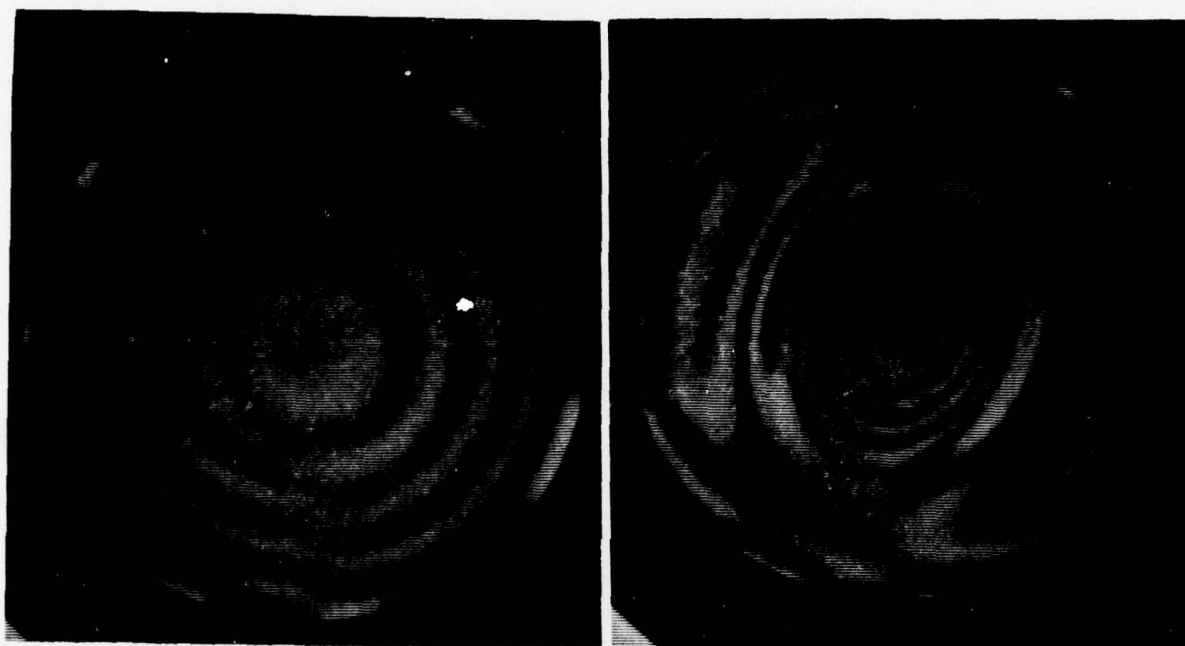
1. Meadows, D. M., Johnson, W. O. and Allen, J. B., "Generation of Surface Contours by Moiré Patterns," Applied Optics, 9 (4), 942-947, 1970.
2. Takasaki, H. "Moiré Topography," Applied Optics, Vol. 9, No. 6, 1476, 1970.
3. Chiang, Fu-Pen, "A Shadow-Moiré Method with Two Discrete Sensitivities," Experimental Mechanics, Vol. 15, No. 10, 382, 1975.
4. Weller, R. and Shepard, B. M., "Displacement Measurement by Mechanical Interferometry," Proceedings SESA, Vol. 6, No. 11, 35, 1948.
5. Theocaris, P. S., "Isopachic Patterns by the Moiré Method," Experimental Mechanics, Vol. 4, No. 6, 153-159, 1968.
6. Theocaris, P. S., "Moiré Pattern of Slope Contours in Flexed Plates," Experimental Mechanics, Vol. 6, No. 4, 115-120, 1966.
7. Dykes, B. C., "Analysis of Displacements in Large Plates by the Grid-Shadow Moiré Technique," Experimental Stress Analysis and Its Influence on Design, "Proc. of the 4th. Int. Conf. on Exp. Str. Analysis", 125-134, 1971.
8. Stromondo, A., Katz, A. and Chiang, F.P., "Mapping Large Deflection of Structures by Moiré Method." Proceedings U.S. Army Solid Mechanics Symp., Ocean City, MD, October 3-5, 1972.
9. Hazell, C. R. and Niven, R. D., "Visualization of Nodes and Antinodes in Vibrating Plates," Experimental Mechanics, 8 (5), 225-231, 1968.
10. Theocaris, P. S., "Moiré Fringes in Strain Analysis," Pergamon Press, 1969, Chap. 7.

11. Powell, R. L. and Stetson, K. A., "Interferometric Vibration Analysis by Wavefront Reconstruction," J. Opt. Soc. Am. 55, 1593, 1965.
12. Hovanesian, J. D. and Hung Y. Y., "Moiré Contour-Sum, Contour-Difference and Vibrational Analysis of Arbitrary Object," Applied Optics, Vol. 10, No. 12, 1971.
13. Vest, C. M. and Sweeney, D. W., "Measurement of Vibrational Amplitude by Modulation of Projected Fringes," Applied Optics, Vol. 11, No. 2, 449, 1972.



0-12

FIGURE 1 SCHEMATIC DIAGRAM OF SHADOW-MOIRÉ METHOD FOR VIBRATION STUDIES



(A)

(B)

0-12

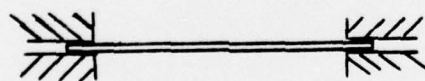
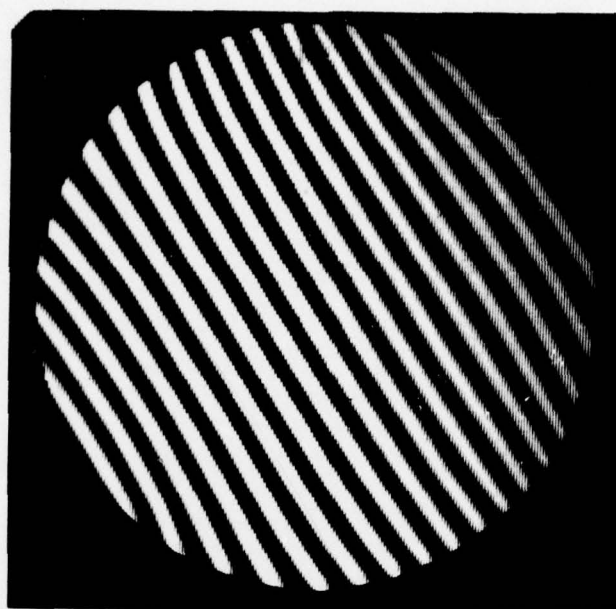
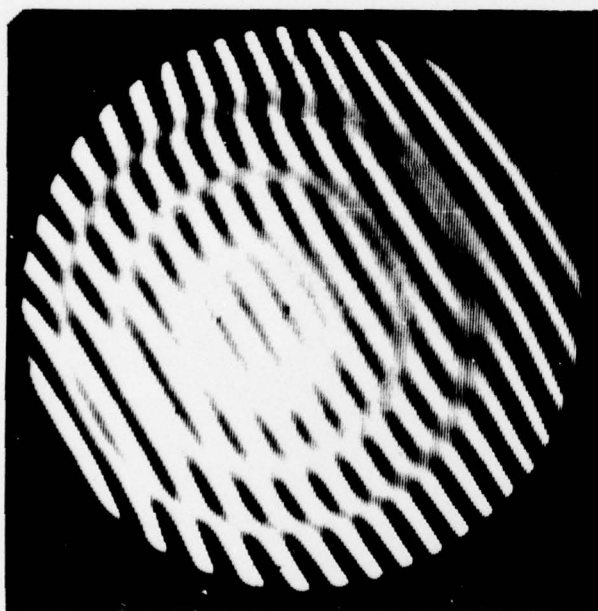


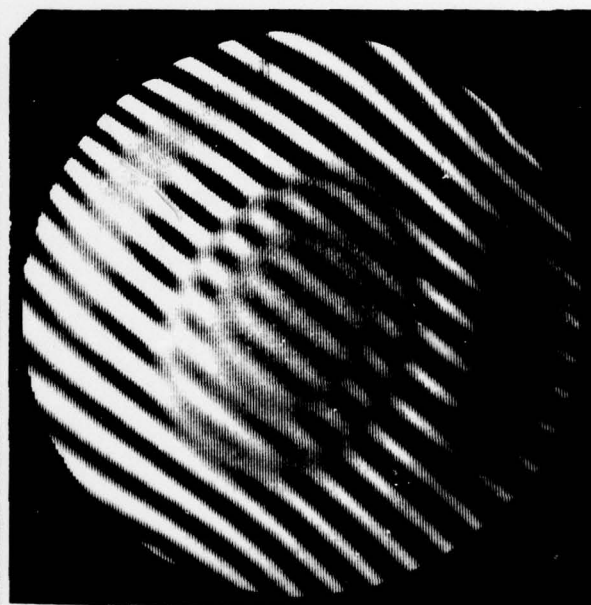
FIGURE 2 FRINGE PATTERN DEPICTING VIBRATIONAL AMPLITUDE OF
A RUBBER MEMBRANE



(A)



(B)



(C)

0-12

FIGURE 3(A) INITIAL FRINGE CARRIER OF THE CIRCULAR, CLAMPED MEMBRANE
 (B) MOIRÉ FRINGE PATTERN DEPICTING VIBRATIONAL AMPLITUDE AT 100 HZ
 (C) MOIRÉ FRINGE PATTERN DEPICTING VIBRATIONAL AMPLITUDE AT 185 HZ

ONR DISTRIBUTION LIST

Part I - Government

Chief of Naval Research
Department of the Navy
Arlington, Virginia 22217
Attn: Code 474 (2)

471
222

Director
ONR Branch Office
495 Summer Street
Boston, Massachusetts 02210

Director
ONR Branch Office
219 S Dearborn Street
Chicago, Illinois 60604

Director
Naval Research Laboratory
Attn: Code 2629 (ONRL)
Washington, D.C. 20390 (6)

U.S. Naval Research Laboratory
Attn: Code 2627
Washington, D.C. 20390

Commanding Officer
ONR Branch Office
207 West 24th Street
New York, N.Y. 10011

Director
ONR Branch Office
1030 E. Green Street
Pasadena, California 91101

Defense Documentation Center
Cameron Station
Alexandria, Virginia 22314 (12)

Army

Commanding Officer
U.S. Army Research Off. Durham
Attn: Mr. J. J. Murray
CRD-AA-IP
Box CM, Duke Station
Durham, North Carolina 27706

Commanding Officer
AMXMR-ATL
Attn: Mr. R. Shea
U.S. Army Materials Res. Agency
Watertown, Massachusetts 02172

Watervliet Arsenal
MAGGS Research Center
Watervliet, New York 12189
Attn: Director of Research

Redstone Scientific Info. Center
Chief, Document Section
U.S. Army Missile Command
Redstone Arsenal, Alabama 35809

Army R & D Center
Fort Belvoir, Virginia 22060

Navy

Commanding Officer & Director
Naval Ship Res. & Dev. Center
Bethesda, Maryland 20034
Attn: Code 042 (Tech. Lib. Br.)

17 (Struc. Mech. Lab.)
172
172
174
177
1800 (Appl. Math. Lab.)
5412S (Dr. W.D. Sette)
19 (Dr. M.M. Sevik)
1901 (Dr. M. Strassberg)
1945
196 (Dr. D. Feit)
1962

Naval Weapons Laboratory
Dahlgren, Virginia 22448

Naval Research Laboratory
Washington, D.C. 20375
Attn: Code 8400
8410
8430
8440
6300
6390
6380

Undersea Explosion Res. Div.
Naval Ship R&D Center
Norfolk Naval Shipyard
Portsmouth, Virginia 23709
Attn: Dr. E. Palmer
Code 780

Naval Ship Res. & Dev. Center
Annapolis Division
Annapolis, Maryland 21402
Attn: Code 2740 - Dr. Y. F. Wang
28 - Mr. R.J. Wolfe
281 - Mr. Niederberger
2814 - Dr. H. Vanderveldt

Technical Library
Naval Underwater Weapons Center
Pasadean Annex
3203 E. Foothill Blvd.
Pasadena, California 91107

U.S. Naval Weapons Center
China Lake, California 93557
Attn: Code 4062 - Mr. W. Werback
4520 - Mr. Ken Bischel

Commanding Officer
U.S. Naval Civil Engr. Lab.
Code L31
Port Hueneme, California 93041

Technical Director
U.S. Naval Ordnance Lab.
White Oak
Silver Spring, Maryland 20910

Technical Director
Naval Undersea R&D Center
San Diego, California 92132

Supervisor of Shipbuilding
U.S. Navy
Newport News, Virginia 23607

Technical Director
Mare Island Naval Shipyard
Vallejo, California 94592

U.S. Navy Underwater Sound Ref.
Lab.

Office of Naval Research
P.O. Box 8337
Orlando, Florida 32806

Chief of Naval Operations
Dept. of the Navy
Washington, D.C. 20350
Attn: Code Op07T

Strategic Systems Project Off.
Department of the Navy
Washington, D.C. 20390
Attn: NSP- 001 Chief Scientist

Deep Submergence Systems
Naval Ship Systems Command
Code 39522
Department of the Navy
Washington, D.C. 203 60

Engineering Dept.
U.S. Naval Academy
Annapolis, Maryland 21402

Naval Air Systems Command
Dept. of the Navy
Washington, D.C. 20360
Attn: NAVAIR 5302 Aero & Struc.
5308 Struc.
52031F Materials
604 Tech. Lib.
320B Struc.

Director, Aero Mechanics
Naval Air Development Center
Johnsville
Warminster, Pennsylvania 18974

Technical Director
U.S. naval Undersea R&D Center
San Diego, California 92132

Engineering Department
U.S. Navla Academy
Annapolis, Maryland 21402

Naval Facilities Engineering Command
Dept. of the Navy
Washington, D.C. 20360
Attn: NAVFAC 03 Res. & Dev.
04 Res. & Dev.
14114 Tech. Lib.

Naval Sea Systems Command
Dept. of the Navy
Washington, D.C. 20360
Attn: NAVSHIP 03 Res. & Tech.
031 Ch. Scientist R&D
03412 Hydromechanics
037 Ship Silencing Div.
035 Weapons Dynamics

Navy cont.

Naval Ship Engineering Center
Prince George's Plaza
Hyattsville, Maryland 20782
Attn: NAVSEC 6100 Ship Sys Engr &

Des Dep
6102C Computer-Aided
Ship Des
6105G
6110 Ship Concept Des
6120 Hull Div.
6120D Hull Div.
6128 Surface Ship
Struct.
6129 Submarine Struct.

Air Force

Commander WADD
Wright-Patterson Air Force Base
Dayton, Ohio 45433
Attn: Code WWRMDD
AFFDL (FDDS)
Structures Division
AFLC (MCEEA)

Chief, Applied Mechanics Group
U.S. Air Force Inst. of Tech.
Wright-Patterson Air Force Base
Dayton, Ohio 45433

Chief, Civil Engineering Branch
WLRC, Research Division
Air Force Weapons Laboratory
Kirtland AFB, New Mexico 87117

Air Force Office of Scientific
Research
1400 Wilson Blvd.
Arlington, Virginia 22209
Attn: Mechanics Div.

NASA

Structures Research Division
National Aeronautics & Space Admin.
Langley Research Center
Langley Station
Hampton, Virginia 23365

National Aeronautic & Space Admin.
Associate Administrator for Ad-
vanced Research & Technology
Washington, D.C. 02546

Scientific & Tech. Info. Facility
NASA Representative (S-AK/DL)
P.O. Box 5700
Bethesda, Maryland 20014

Other Government Activities

Commandant
Chief, Testing & Development Div.
U.S. Coast Guard
1300 E. Street, N.W.
Washington, D.C. 20226

Technical Director
Marine Corps Dev & Educ. Command
Quantico, Virginia 22134

Director
National Bureau of Standards
Washington, D.C. 20234
Attn: Mr. E.L. Wilson, EN 219

Dr. M. Gaus
National Science Foundation
Engineering Division
Washington, D.C. 20550

Science & Tech. Division
Library of Congress
Washington, D.C. 20540

Director
Defense Nuclear Agency
Washington, D.C. 20305
Attn: SPSS

Commander Field Command
Defense Nuclear Agency
Sandia Base
Albuquerque, New Mexico 87115

Director Defense Research & Engr
Technical Library
Room 3C-128
The Pentagon
Washington, D.C. 20301

Chief, Airframe & Equipment Branch
FS-120
Office of Flight Standards
Federal Aviation Agency
Washington, D.C. 20553

Chief, Research and Development
Maritime Administration
Washington, D.C. 20235

Deputy Chief, Office of Ship Constr.
Maritime Administration
Washington, D.C. 20235
Attn: Mr. U.L. Russo

Atomic Energy Commission
Div. of Reactor Devel. & Tech.
Germantown, Maryland 20767

Ship Hull Research Committee
National Research Council
National Academy of Sciences
2101 Constitution Avenue
Washington, D.C. 20418
Attn: Mr. A.R. Lytle

Part 2 - Contractors and Other
Technical Collaborators

Universities

Dr. J. Tinsley Oden
University of Texas at Austin
345 Eng. Science Bldg.
Austin, Texas 78712

Prof. Julius Miklowitz
California Institute of Technology
Div. of Engineering & Applied Sci.
Pasadena, California 91109

Dr. Harold Liebowitz, Dean
School of Engr. & Applied Science
George Washington University
725 - 23rd St., N.W.
Washington, D.C. 20006

Prof. Eli Sternberg
California Institute of Technology
Div. of Engr. & Applied Sciences
Pasadena, California 91109

Prof. Paul M. Naghdi
University of California
Div. of Applied Mechanics
Etcheverry Hall
Berkeley, California 94720

Professor P.S. Symonds
Brown University
Division of Engineering
Providence, R.I. 02912

Prof. A.J. Durelli
The Catholic University of America
Civil/Mechanical Engineering
Washington, D.C. 20017

Prof. R.B. Testa
Columbia University
Dept. of Civil Engineering
S.W. Mudd Bldg.
New York, New York 10027

Prof. H.H. Bleich
Columbia University
Dept. of Civil Engineering
Amsterdam & 120th St.
New York, New York 10027

Prof. F.L. DiMaggio
Columbia University
Dept. of Civil Engineering
616 Mudd Building
New York, New York 10027

Prof. A.M. Freudenthal
George Washington University
School of Engineering & Applied
Science
Washington, D.C. 20006

D.C. Evans
University of Utah
Computer Science Division
Salt Lake City, Utah 84112

Prof. Norman Jones
Massachusetts Inst. of Technology
Dept. of Naval Architecture &
Marine Engrng
Cambridge, Massachusetts 02139

Professor Albert I. King
Biomechanics Research Center
Wayne State University
Detroit, Michigan 48202

Dr. V.R. Hodgson
Wayne State University
School of Medicine
Detroit, Michigan 48202

Universities cont.

Dean B.A. Boley
Northwestern University
Technological Institute
2145 Sheridan Road
Evanston, Illinois 60201

Prof. P.G. Hodge, Jr.
University of Minnesota
Dept. of Aerospace Engng & Mech.
Minneapolis, Minnesota 55455

Dr. D.C. Drucker
University of Illinois
Dean of Engineering
Urbana, Illinois 61801

Prof. N.M. Newmark
University of Illinois
Dept. of Civil Engineering
Urbana, Illinois 61801

Prof. E. Reissner
University of California, San Diego
Dept. of Applied Mechanics
La Jolla, California 92037

Prof. William A. Nash
University of Massachusetts
Dept. of Mechanics & Aerospace Eng.
Amherst, Massachusetts 01002

Library (Code 0384)
U.S. Naval Postgraduate School
Monterey, California 93940

Prof. Arnold Allentuch
Newark College of Engineering
Dept. of Mechanical Engineering
323 High Street
Newark, New Jersey 07102

Dr. George Herrmann
Stanford University
Dept. of Applied Mechanics
Stanford, California 94305

Prof. J.D. Achenbach
Northwestern University
Dept. of Civil Engineering
Evanston, Illinois 60201

Director, Applied Research Lab.
Pennsylvania State University
P.O. Box 30
State College, Pennsylvania 16801

Prof. Eugen J. Skudrzyk
Pennsylvania State University
Applied Research Laboratory
Dept. of Physics - P.O. Box 30
State College, Pennsylvania 16801

Prof. J. Kempner
Polytechnic Institute of Brooklyn
Dept. of Aero. Engrg & Applied Mech.
333 Jay Street
Brooklyn, N.Y. 11201

Prof. J. Klosner
Polytechnic Institute of Brooklyn
Dept. of Aerospace & Appl. Mech.
333 Jay Street
Brooklyn, N.Y. 11201

Prof. R.A. Schapery
Texas A&M University
Dept. of Civil Engineering
College Station, Texas 77840

Prof. W.D. Pilkey
University of Virginia
Dept. of Aerospace Engineering
Charlottesville, Virginia 22903

Dr. H.G. Schaeffer
University of Maryland
Aerospace Engineering Dept.
College Park, Maryland 20742

Prof. K.D. Willmert
Clarkson College of Technology
Dept. of Mechanical Engineering
Potsdam, N.Y. 13676

Dr. J.A. Stricklin
Texas A&M University
Aerospace Engineering Dept.
College Station, Texas 77843

Dr. L.A. Schmit
University of California, LA
School of Engineering & Applied Sci.
Los Angeles, California 90024

Dr. H.A. Kamel
The University of Arizona
Aerospace & Mech. Engineering Dept.
Tucson, Arizona 85721

Dr. B.S. Berger
University of Maryland
Dept. of Mechanical Engineering
College Park, Maryland 20742

Prof. G.R. Irwin
Dept. of Mechanical Engng.
University of Maryland
College Park, Maryland 20742

Dr. S.J. Fenves
Carnegie-Mellon University
Dept. of Civil Engineering
Schenley Park
Pittsburgh, Pennsylvania 15213

Dr. Ronald L. Huston
Dept. of Engineering Analysis
Mail Box 112
University of Cincinnati
Cincinnati, Ohio 45221

Prof. George Sih
Dept. of Mechanics
Lehigh University
Bethlehem, Pennsylvania 18015

Prof. A.S. Kobayashi
University of Washington
Dept. of Mechanical Engineering
Seattle, Washington 98105

Librarian
Webb Institute of Naval Architecture
Crescent Beach Road, Glen Cove
Long Island, New York 11542

Prof. Daniel Frederick
Virginia Polytechnic Institute
Dept. of Engineering Mechanics
Blacksburg, Virginia 24061

Prof. A.C. Eringen
Dept. of Aerospace & Mech. Sciences
Princeton University
Princeton, New Jersey 08540

Dr. S.L. Koh
School of Aero., Astro. & Eng. Sc.
Purdue University
Lafayette, Indiana 47907

Prof. E.H. Lee
Div. of Engrg. Mechanics
Stanford University
Stanford, California 94305

Prof. R.D. Mindlin
Dept. of Civil Engrg
Columbia University
S.W. Mudd Building
New York, N.Y. 10027

Prof. S.B. Dong
University of California
Dept. of Mechanics
Los Angeles, California 90024

Prof. Burt Paul
University of Pennsylvania
Towne School of Civil & Mech Engr
Rm. 113 - Towne Building
220 S. 33rd Street
Philadelphia, Pennsylvania 19104

Prof. J.W. Liu
Dept. of Chemical Engr. & Metal.
Syracuse University
Syracuse, N.Y. 13210

Prof. S. Bodner
Technion R&D Foundation
Haifa, Israel

Prof. R.J.H. Bollard
Chairman, Aeronautical Engr. Dept.
207 Guggenheim Hall
University of Washington
Seattle, Washington 98105

Prof. G.S. Heller
Division of Engineering
Brown University
Providence, Rhode Island 02912

Prof. Werner Goldsmith
Dept. of Mechanical Engineering
Div. of Applied Mechanics
University of California
Berkeley, California 94720

Prof. J.R. Rice
Division of Engineering
Brown University
Providence, R.I. 02912

Prof. R.S. Rivlin
Center for the Application of
Mathematics
Lehigh University
Bethlehem, Pennsylvania 18015

Library (code 0384)
U.S. Naval Postgraduate School
Monterey, California 93940

Dr. Francis Cozzarelli
Div. of Interdisciplinary
Studies & Research
School of Engineering
State University of New York
Buffalo, N.Y. 14214

Industry and Research Institutes

Library Services Dept.
Report Section Bldg. 14-14
Argonne National Laboratory
9700 S. Cass Avenue
Argonne, Illinois 60440

Dr. M.C. Junger
Cambridge Acoustical Associates
129 Mount Auburn St.
Cambridge, Massachusetts 02138

Dr. L.H. Chen
General Dynamics Corporation
Electric Boat Division
Groton, Connecticut 06340

Dr. J.E. Greenspon
J.G. Engineering Research Assoc.
3831 Menlo Drive
Baltimore, Maryland 21215

Dr. S. Batdorf
The Aerospace Corp.
P.O. Box 92957
Los Angeles, California 90009

Dr. K.C. Park
Lockheed Palo Alto Research Lab.
Dept. 5233, Bldg. 205
3251 Hanover St.
Palo Alto, CA 94304

Library
Newport News Shipbuilding & Dry
Dock Company
Newport News, Virginia 23607

Dr. W.F. Bozich
McDonnell Douglas Corporation
5301 Bolsa Avenue
Huntington Beach, CA 92647

Dr. H.N. Abramson
Southwest Research Institute
Technical Vice President
Mechanical Sciences
P.O. Drawer 28510
San Antonio, Texas 78284

Dr. R.C. DeHart
Southwest Research Institute
Dept. of Structural Research
P.O. Drawer 28510
San Antonio, Texas 78284

Dr. M.L. Baron
Weidlinger Associates, Consulting
Engineers
110 East 59th Street
New York, N.Y. 10022

Dr. W.A. Rieseemann
Sandia Laboratories
Sandia Base
Albuquerque, New Mexico 87115

Dr. T.L. Geers
Lockheed Missiles & Space Co.
Palo Alto Research Laboratory
3251 Hanover Street
Palo Alto, California 94304

Dr. J.L. Tocher
Boeing Computer Services, Inc.
P.O. Box 24346
Seattle, Washington 98124

Mr. William Caywood
Code BBE, Applied Physics Laboratory
8621 Georgia Avenue
Silver Spring, Maryland 20034

Mr. P.C. Durup
Lockheed-California Company
Aeromechanics Dept., 74-43
Burbank, California 91503

Assistant Chief for Technology
Office of Naval Research, Code 200
Arlington, Virginia 22217

UNCLASSIFIED

SECURITY CLASSIFICATION OF THIS PAGE (When Data Entered)

REPORT DOCUMENTATION PAGE		READ INSTRUCTIONS BEFORE COMPLETING FORM
1. REPORT NUMBER 39	2. GOVT ACCESSION NO.	3. RECIPIENT'S CATALOG NUMBER
4. TITLE (and Subtitle) Time-Averaged Shadow-Moire Method for Studying Vibrations		5. TYPE OF REPORT & PERIOD COVERED
7. AUTHOR(s) Y. Y. Hung, C. Y. Liang, J. D. Hovanesian and A. J. Durelli		6. PERFORMING ORG. REPORT NUMBER 39479
9. PERFORMING ORGANIZATION NAME AND ADDRESS Oakland University Rochester, Mi. 48063		8. CONTRACT OR GRANT NUMBER(s) N-00014-76-C-0487 new
11. CONTROLLING OFFICE NAME AND ADDRESS Office of Naval Research Department of the Navy Washington, D.C. 20025		10. PROGRAM ELEMENT, PROJECT, TASK AREA & WORK UNIT NUMBERS
14. MONITORING AGENCY NAME & ADDRESS (if different from Controlling Office)		12. REPORT DATE November, 1976
		13. NUMBER OF PAGES 25
		15. SECURITY CLASS. (of this report) Unclassified
		15a. DECLASSIFICATION/DOWNGRADING SCHEDULE
16. DISTRIBUTION STATEMENT (of this Report) Distribution of this report is unlimited.		
17. DISTRIBUTION STATEMENT (of the abstract entered in Block 20, if different from Report)		
18. SUPPLEMENTARY NOTES		
19. KEY WORDS (Continue on reverse side if necessary and identify by block number) Moire vibrations plates time-averaged		
20. ABSTRACT (Continue on reverse side if necessary and identify by block number) A time-averaged shadow-moire method is presented which permits the determination of the amplitude distribution of the deflection of a plate in steady state vibration. No stroboscope is required and the recording is done statically. The method is less sensitive than holographic methods and is therefore suitable for studying relatively large amplitudes.		

DD FORM 1 JAN 73 1473

EDITION OF 1 NOV 65 IS OBSOLETE
S/N 0102-014-6601

Unclassified

SECURITY CLASSIFICATION OF THIS PAGE (When Data Entered)